Virology 433 (2012) 449–461

Contents lists available at SciVerse ScienceDirect

Virology

journal homepage: www.elsevier.com/locate/yviro

Alfalfa mosaic virus replicase proteins, P1 and P2, localize to the tonoplast in the presence of virus RNA

Amr Ibrahim [a,c], Heather M. Hutchens [a], R. Howard Berg [b], L. Sue Loesch-Fries [a,*]

[a] Department of Botany and Plant Pathology, Purdue University, West Lafayette, IN 47907, USA
[b] Integrated Microscopy Facility, Donald Danforth Plant Science Center, Saint Louis, MO 63132, USA
[c] Present address: Genomics Facility, Agricultural Genetic Engineering Research Institute, Agricultural Research Center, Giza 12619, Egypt

ARTICLE INFO

Article history:
Received 8 May 2012
Returned to author for revisions
1 August 2012
Accepted 7 August 2012
Available online 19 September 2012

Keywords:
Alfalfa mosaic virus
RNA virus
Virus replication complex
Localization of virus proteins
Endosome
Multivesicular body
Tonoplast
Prevacuolar compartment

ABSTRACT

To identify the virus components important for assembly of the Alfalfa mosaic virus replicase complex, we used live cell imaging of *Arabidopsis thaliana* protoplasts that expressed various virus cDNAs encoding native and GFP-fusion proteins of P1 and P2 replicase proteins and full-length virus RNAs. Expression of P1-GFP alone resulted in fluorescent vesicle-like bodies in the cytoplasm that colocalized with FM4-64, an endocytic marker, and RFP-AtVSR2, RabF2a/Rha1-mCherry, and RabF2b/Ara 7-mCherry, all of which localize to multivesicular bodies (MVBs), which are also called prevacuolar compartments, that mediate traffic to the lytic vacuole. GFP-P2 was driven from the cytosol to MVBs when expressed with P1 indicating that P1 recruited GFP-P2. P1-GFP localized on the tonoplast, which surrounds the vacuole, in the presence of infectious virus RNA, replication competent RNA2, or P2 and replication competent RNA1 or RNA3. This suggests that a functional replication complex containing P1, P2, and a full-length AMV RNA assembles on MVBs to traffic to the tonoplast.

Introduction

All plus-strand viruses replicate on membranes that differ in origin and location, which provide a lipid-rich platform on which virus and host proteins assemble into replication complexes (Stapleford and Miller, 2010; den Boon and Ahlquist, 2010; Nagy and Pogany, 2012). These complexes are on the endoplasmic reticulum (ER) and ER-derived membranes for *Hepatitis C virus* (HCV) (Egger et al., 2002; Gosert et al., 2003; Targett-Adams et al., 2008), *Brome mosaic virus* (BMV) (Restrepo-Hartwig and Ahlquist, 1996; Schwartz et al., 2002), *Tobacco mosaic virus* (TMV) (Heinlein et al., 1998; Más and Beachy (1999)), and *Cowpea mosaic virus* (Carette et al., 2000), on mitochondria for *Flock house virus* (Miller et al., 2001), peroxisomes for *Tomato bushy stunt virus* (TBSV) (McCartney et al., 2005), and chloroplast membranes for *Turnip yellow mosaic virus* (TYMV) (Hatta et al., 1973). Alternatively, membranes in the endocytic pathway are used for replication by a number of viruses. For example, lysosomal and endosomal membranes are remodeled for replication by *Rubella virus* (Magliano et al., 1998; Kujala et al., 1999) and *Semliki Forest virus* (SFV) (Froshauer et al., 1988; Salonen et al., 2003; Spuul et al., 2010). Similarly, the vacuolar membrane of plants, which is equivalent to the lysosomal membranes of animals, serves as the site of replication of *Cucumber mosaic virus* (CMV) (Cillo et al., 2002) and *Tomato aspermy virus* (Hatta and Francki, 1981).

The formation of viral replication complexes and their targeting to specific membranes has been studied for a number of viruses. Often, one of the virus replicase proteins has affinity for a specific membrane upon which the complex assembles. For example, the replicase protein, 1a, of BMV targets the perinuclear ER where it induces spherules on the membrane to house the enzymes and templates for RNA replication (Restrepo-Hartwig and Ahlquist, 1996, 1999; den Boon et al., 2001; Schwartz et al., 2002). 1a recruits the viral RNA polymerase, 2a, the viral RNAs, and host proteins such as reticulon proteins required for spherule formation (Chen and Ahlquist, 2000; Wang et al., 2005; Diaz et al., 2010). The TYMV 160K replicase protein and the TBSV p33 replicase protein are also master organizers of replicase complex formation (Prod'homme et al., 2003; McCartney et al., 2005).

The genome organization of *Alfalfa mosaic virus* (AMV) is similar to other tripartite positive-sense RNA viruses such as BMV and CMV. AMV, the single member of the *Alfamovirus* genus in the family *Bromoviridae*, has three capped and non-polyadenylated genomic RNAs (RNA1–3). RNA1 encodes P1, which contains putative helicase and a methyltransferase domains; RNA2 encodes P2, the RNA-dependent RNA polymerase.

* Corresponding author. Fax: +1 765 4940363.
E-mail address: loeschfr@purdue.edu (L. Sue Loesch-Fries).

0042-6822/$ - see front matter © 2012 Elsevier Inc. All rights reserved.
http://dx.doi.org/10.1016/j.virol.2012.08.018

RNA3 is bicistronic in that it encodes P3, the movement protein, and the coat protein (CP); however, only P3 is translated from RNA3. The CP is translated from a subgenomic RNA, RNA4, which is synthesized during the replication of RNA3 (Smit and Jaspars, 1982) and is encapsidated into virions. Viruses in the *Alfamovirus* and the *Ilarvirus* genera are unique in that they require the virus CP or RNA4 for infection (Gonsalves and Garnsey, 1975; Alblas and Bol, 1978). The AMV CP has strong affinity for the virus RNA so that the N-terminal 26 amino acids of CP binding strongly to the 3′ end of all AMV RNAs resulting in significant changes in the RNA conformation (Guogas et al., 2004). Alternative mechanisms have been suggested to explain the role of the CP. One proposal is that the CP enhances viral translation based on the finding that translation is enhanced by polyadenylation of the non-polyadenylated AMV RNAs and that the CP interacts with eIF4G subunit of the initiation complex (Neeleman et al., 2001; Krab et al., 2005). Another proposal suggests that CP-RNA cofolding generates a unique structure for binding of the virus replicase (Guogas et al., 2004).

AMV P1 and P2 replicase proteins interact in vitro and in yeast two-hybrid assays (Van Der Heijden et al., 2001). Expression of these proteins from full-length AMV RNA1 and 2 transgenes in tobacco plants is sufficient for the assembly of replicase complexes that synthesize minus-strands of RNA1 and 2 (Thole et al., 2001). However, the expression of RNA3 encoding the CP is required for plus-strand RNA synthesis. Additional studies indicated that the assembly of an active replicase also requires the presence of virus RNA 3′ ends (Vlot et al., 2001). The replication complex likely resides on the tonoplast where P1 and P2 were shown to colocalize in AMV-infected protoplasts (Van Der Heijden et al., 2001).

AMV replicates efficiently in arabidopsis protoplasts and infection can be launched from AMV cDNAs (Balasubramaniam et al., 2006). Here, we investigated the sub-cellular location of replication competent P1 and P2 GFP-fusion proteins in arabidopsis protoplasts following transfection with cDNA or AMV RNA. Results from confocal microscopy of live protoplasts confirmed that P1 and P2 associate with the tonoplast during infection. However, when expressed alone, P1 fusion protein colocalizes with proteins specific to multivesicular bodies (MVBs), which are also called prevacuolar compartments, and when expressed with P2, it recruits P2 to the MVBs. With the coexpression of at least one of any of the full-length AMV RNAs and P2, P1-GFP associates with the tonoplast. This suggests that the formation of an active replicase complex containing P1, P2, and full-length RNA is required for transport of the complex to the tonoplast via MVBs.

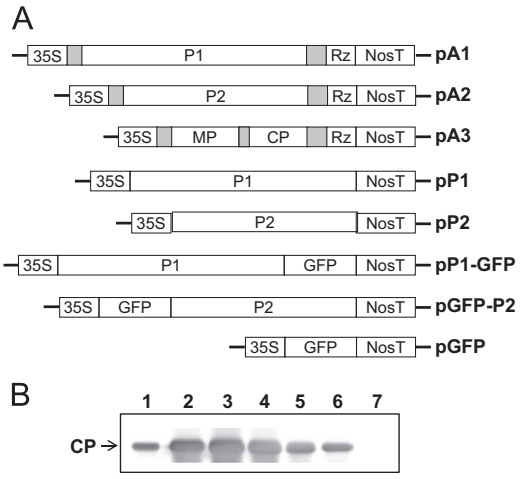

Fig. 1. AMV cDNA constructs infect arabidopsis protoplasts. (A) cDNA constructs used for the expression of AMV RNA and proteins in protoplasts. In all constructs: boxes labeled with 35S denote the Cauliflower mosaic virus (CaMV) 35S promoter sequence, boxes labeled with NosT denote the nopaline synthase termination sequence, boxes labeled with Rz denote the ribozyme sequence of *Hepatitis delta virus*. Boxes labeled with P1, P2, MP, or CP denote sequences encoding AMV proteins or the green fluorescent protein (GFP). The shaded boxes represent AMV RNA untranslated regions. cDNAs for transcription of full-length virus RNAs contained Hepatitis delta virus ribozyme sequences at the 3′ end of the virus sequences so that exact full-length RNAs with no extra nucleotides would be produced in the cytoplasm, whereas the constructs for protein synthesis contained only the ORFs without the ribozyme sequence. (B) Western blot analysis of CP accumulation in arabidopsis protoplasts transfected with mixtures of cDNAs. Samples contained total protein from 2.5×10^4 protoplasts 24 h following transfection with: lane 2, pA1, pA2, pA3; lane 3, pP1, pA2, pA3; lane 4, pA1, pP2, pA3; lane 5, pA1, pGFP-P2, pA3; lane 6, pP1-GFP, pA2, pA3; lane 7, no DNA (mock transfection). Lane 1 contains AMV CP translated in vitro (arrow).

Results

P1 and P2 GFP fusion proteins were functional in virus replication

AMV cDNAs under control of the 35S promoter (pA1-35S, pA2-35S, and pA3-35S for the expression of AMV RNA1, 2, and 3, respectively) were previously shown to be infectious upon transfection of arabidopsis protoplasts resulting in the synthesis of AMV RNAs, which subsequently replicate producing an infection similar to wild type virions (Balasubramaniam et al., 2006). These cDNAs (renamed pA1, pA2, and pA3) were used with the new constructs containing only P1 and P2 ORFs with or without fusion to GFP to investigate the location of the replicase proteins in arabidopsis protoplasts. pP1 and pP2 and their tagged constructs were used for the expression of P1 and P2 proteins without virus infection. To determine if the proteins encoded by the new constructs (Fig. 1A) were functional in replication, the constructs encoding P1 and P2 were mixed with pA2 and pA3 or with pA1 and pA3, respectively for transfection. If the P1 and P2 proteins were functional, the full-length RNAs transcribed from pA1, pA2, or pA3 would be replicated and CP would accumulate, which occurs only when subgenomic RNA4 is made during the replication of RNA3. Fig. 1B shows that pP1 (lane 3) and pP2 (lane 4) along with pA3 enabled the translation and accumulation of AMV CP. These samples contained about as much CP as did samples transfected with pA1, pA2, and pA3 (Fig. 1B, lane 2). This indicates that P1 and P2 enabled the replication of transcribed RNA3. Constructs containing P1 and P2 ORFs fused to the GFP ORF (Fig. 1A) were likewise tested for function. Both pP1-GFP and pGFP-P2 enabled the accumulation of CP (Fig. 1B, lane 6 and lane 5, respectively); however, the fusion proteins were less effective in replication than P1 and P2 (compare lanes 3 and 4 with lanes 5 and 6) and pP1-GFP was less effective than GFP-P2 (compare lane 6 with lane 5). Therefore, in an effort to increase function of the P1 fusion protein, a second construct was made to express a P1 fusion protein with GFP at the N-terminus. However, GFP-P1 encoded by this construct was unable to participate in RNA3 replication. CP did not accumulate in protoplasts transfected with a mixture of pGFP-P1, pA2, and pA3 (data not shown). Therefore, only pP1-GFP was used in all experiments. Immunoassays of protoplasts transfected with AMV cDNAs and pP1-GFP or pGFP-P2 indicated that CP accumulated in 11–14% or 16–29% of protoplasts, respectively. This was sufficient to observe the behavior of the fusion proteins by live cell imaging.

When expressed alone, P1-GFP colocalized with FM4-64

Protoplasts were transfected with pP1-GFP to determine the location of P1-GFP when expressed alone. Fluorescence was first

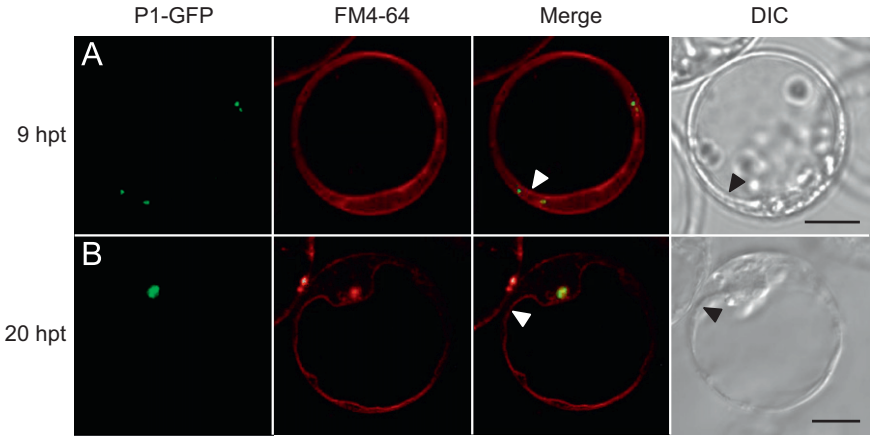

Fig. 2. P1-GFP accumulates in punctate bodies that colocalize with FM4-64. Arabidopsis protoplasts were transfected with 5 μg of pP1-GFP and continuously incubated with FM4-64 at 10 μM for the indicated amounts of time post transfection (hpt) and immediately imaged. Each row contains images of single optical sections of 0.44 μm thickness. Images of P1-GFP are in the green channel, FM4-64 is in the red channel, and the merged images are to the right. DIC images are at the far right. The arrowheads indicate the positions of the tonoplast. Scale bars = 10 μm. (For interpretation of the references to color in this figure legend, the reader is referred to the web version of this article.)

detectable about 5 h post transfection (hpt) in a few protoplasts and it increased in intensity and frequency over time. The fluorescence was observable as small punctate spots (Fig. 2A). These spots colocalized with FM4-64, a lipophylic dye that is selective for membranes in the endocytic pathway from the plasma membrane to the membrane of the vacuole, the tonoplast, and is used to investigate vesicle trafficking in living cells (Bolte et al., 2004; Griffing, 2008; Van Gisbergen et al., 2008). The protoplast shown in Fig. 2A was labeled continuously with FM4-64 after transfection so that FM4-64 is visible on the plasma membrane, endosome and MVB membranes, and the tonoplast. The DIC image is at the right and arrowheads point to the tonoplast. When protoplasts were observed at longer intervals after transfection, large fluorescent bodies could be detected (Fig. 2B). The fluorescent body colocalized with a large structure marked by FM4-64 and it is close but separate from the tonoplast, which is also labeled with FM4-64. The number of fluorescent bodies increased and became larger with time, sometimes appearing as complexes of numerous small bodies. However, all colocalized with FM4-64l. Van Der Heijden et al. (2001) reported that AMV P1 was exclusively on the tonoplast in protoplasts made from infected cells. Therefore, to determine whether transfection using 5 μg of pP1-GFP caused artifacts due to excessive protein expression, protoplasts were transfected with 0.5 to 10 μg of plasmid so that individual protoplasts received either a few copies of pP1-GFP or many copies. The frequency of protoplasts with observable fluorescent bodies decreased with decreasing plasmid; however, the fluorescence was still observable as punctate bodies with small amounts of plasmid or as larger bodies with greater amounts of plasmid similar to the bodies shown in Fig. 2. Therefore, the pattern of P1-GFP localization was not an artifact due to the accumulation of large amounts of P1-GFP. Colocalization with FM4-64 suggested that P1-GFP accumulated on organelles in the endocytic pathway.

P1-GFP localized to MVBs

To determine whether P1-GFP accumulated on organelles that are not part of the endocytic pathway, we expressed P1-GFP with a number of cellular markers. The location of chloroplasts was detected by chlorophyll autofluorescence in protoplasts transfected with pP1-GFP. However, the signal from P1-GFP did not colocalize with chloroplasts indicating that P1-GFP did not accumulate on the chloroplast membrane (Fig. 3A). To detect the endoplasmic reticulum, we co-transfected protoplasts with pP1-GFP and pER-rk (Nelson et al., 2007), which encodes the signal peptide of arabidopsis wall-associated kinase 2 (He et al., 1999) fused to mCherry followed by the ER retention signal (Gomord and Denmat, 1997). The ER-targeted protein formed a network throughout the cytoplasm (Fig. 3B); however, P1-GFP did not colocalize with this protein indicating that P1-GFP was not associated with the ER network. To detect peroxisomes, we co-transfected protoplasts with pP1-GFP and ppx-rk (Nelson et al., 2007), which encodes the peroxisomal targeting signal 1 fused to mCherry. Many punctate spots of mCherry accumulated (Fig. 3C); however, P1-GFP did not colocalize with them. This indicates that P1-GFP did not accumulate on peroxisomes.

P1-GFP always colocalized with FM4-64. Therefore, we compared the distribution pattern of P1-GFP to that of proteins that reside in the endocytic pathway and colocalize with FM4-64: soybean α-1, 2-mannosidease, GmMan1, (Saint-Jore-Dupas et al., 2004), which localizes in the Golgi, RabA4b (Preuss et al., 2004), which localizes in a unique trans-Golgi network (TGN) compartment involved in secretion, and three proteins, which localize to MVBs involved in transport to the lytic vacuole including: AtVSR2 (Miao et al., 2006), RabF2a (Sohn et al., 2003), and RabF2b (Lee et al., 2004). pG-rk, which encodes the first 49 amino acids of GmMan1 including the cytoplasmic tail and transmembrane domain fused to mCherry (Nelson et al., 2007) was used for transfection along with pP1-GFP. The marker accumulated throughout the cytoplasm in numerous punctate spots (Fig. 4A). P1-GFP also accumulated in punctate spots, but none colocalized with mCherry-GmMan1 on the Golgi. Similarly, P1-GFP did not colocalize with mRFP-RabA4b (Fig. 4B). These results indicate that P1-GFP did not localize on the Golgi marked by GmMan1 or on the TGN-like compartment marked by RabA4b. Co-localization of P1-GFP, however, occurred with the three proteins that reside on MVBs (Lam et al., 2007; Miao et al., 2008). P1-GFP colocalized with the fusion proteins of two mammalian Rab5 homologues, RabF2a (Fig. 4C) and RabF2b (Fig. 4D). It also colocalized with the vacuolar sorting receptor protein, AtVSR2, which is an arabidopsis homologue of vacuolar sorting receptor BP-80 identified in pea plants (Fig. 4E). In all of the protoplasts that expressed both P1-GFP and MVB-specific proteins, P1-GFP fluorescence always colocalized with the MVB marker. In Fig. 4C, all visible MVBs are marked with both P1-GFP and RabF2a-mCherry. Generally, however,

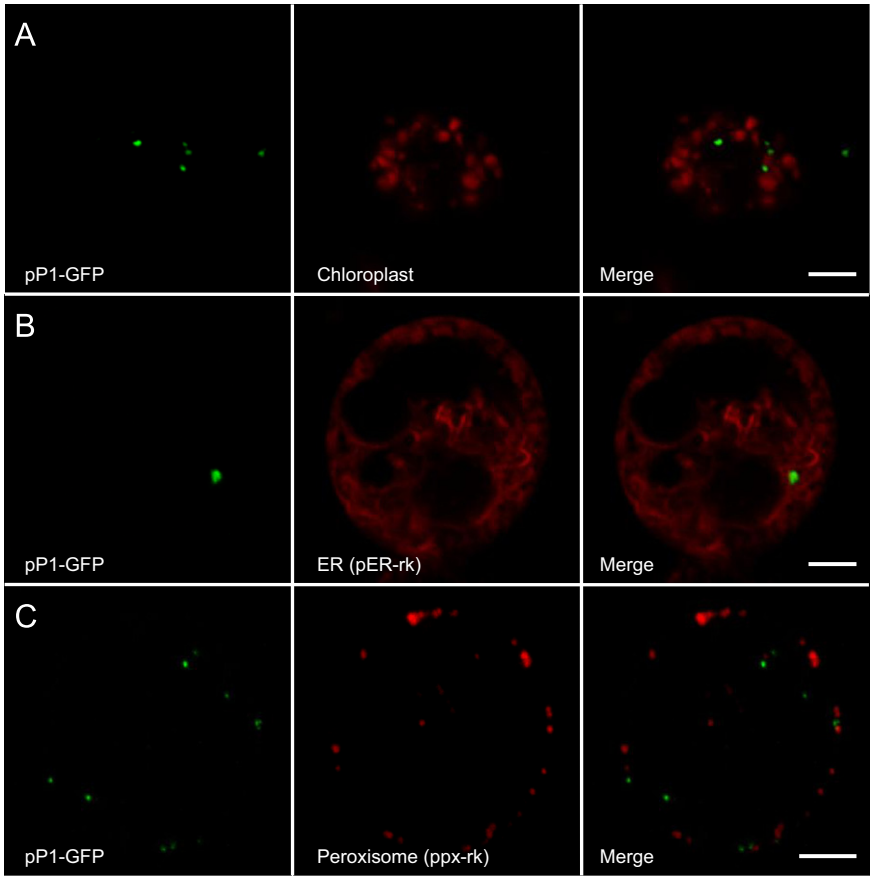

Fig. 3. P1-GFP does not accumulate on chloroplasts, ER, or peroxisomes. Projection images of arabidopsis protoplasts transfected with (A) pP1-GFP alone (9 optical sections) for detection of chloroplasts in the red channel, (B) pP1-GFP and pER-rk, which encodes a protein targeted to the endoplasmic reticulum, (9 optical sections) or (C) pP1-GFP and ppx-rk, which encodes a protein targeted to peroxisomes, (15 optical sections). Images are labeled with the transfection plasmid, pP1-GFP, in the green channel or with the detected host organelle and transfection plasmid in the red channel. Images were collected from 24–30 hpt. Merged images are to the right. Scale bars = 10 μm. (For interpretation of the references to color in this figure legend, the reader is referred to the web version of this article.)

protoplasts contained a portion of MVBs labeled only with the specific marker, which indicated that P1-GFP did not reside on all of the observable MVBs as shown in Fig. 4D and E. Our results, therefore, indicate that P1-GFP localizes to MVBs that are in the pathway to the lytic vacuole (Record and Griffing, 1988).

GFP-P2 was distributed throughout the cytosol when expressed alone, but was recruited to MVBs when expressed with P1

Transfection of arabidopsis protoplasts with pGFP-P2 resulted in fluorescence throughout the cytosol as delimited by the tonoplast marked by FM4-64 (Fig. 5A). The distribution was similar to GFP (Fig. 5B) except that GFP-P2 never accumulated in the nucleus, which is located to the left in Fig. 5A and above the faintly marked tonoplast in Fig. 5B. P1 and P2 have been shown to interact in vitro and in vivo (Van Der Heijden et al., 2001; Reichert et al., 2007). To determine if this interaction affects the distribution of either protein in vivo, we transfected protoplasts with mixtures of pP1-GFP and pP2 or pP1 and pGFP-P2. The presence of P2 did not affect the localization of P1-GFP (Fig. 5C). Here, GFP fluorescence was observable on large bodies that were marked by FM4-64. GFP-P2 distribution in the protoplasts, however, was markedly influenced by P1. Fluorescence accumulated on discrete bodies, which were labeled with FM4-64 as shown in Fig. 5D. The bodies were identical to those that accumulated upon the expression of P1-GFP alone such as in Fig. 2. Generally, there was faint diffuse fluorescence in the cytosol, such as in Fig. 5D. Thus, not all of the GFP-P2 colocalized with P1 in a distribution similar to that observed in infected protoplasts (Van Der Heijden et al., 2001). Coexpression of GFP-P2 and P1 with RabF2a-mCherry in protoplasts indicated that GFP-P2 and RabF2a-mCherry colocalized (Fig. 5E). Faint GFP fluorescence in the cytosol in Fig. 5E indicates that some GFP-P2 remained in the cytosol as in Fig. 5D. Therefore, P1 recruited GFP-P2 to MVBs marked by RabF2a-mCherry on which P1 localized when expressed alone.

P1-GFP localized to the tonoplast when expressed with AMV RNAs or cDNAs

P1 and P2 were detected on tonoplasts in infected cowpea protoplasts (Van Der Heijden et al., 2001), but in our studies neither P1 nor P2 separately or together accumulated on tonoplasts. To determine whether infection would alter the localization of the replicase proteins, we included AMV RNAs 1–4, which had been isolated from virions, in the transfection mixture containing pP1-GFP. The RNAs rapidly replicated in the presence of P1-GFP so that at 10 hpt, 77–96% of the protoplasts were infected as determined by an immunofluorescent assay for AMV CP. In all protoplasts, fluorescence was detected on the tonoplast and some protoplasts contained bright MVBs as well (Fig. 6A and B). All fluorescence colocalized with FM4-64, which in Fig. 6A is marking the tonoplast and a large MVB, whereas in Fig. 6B, it is

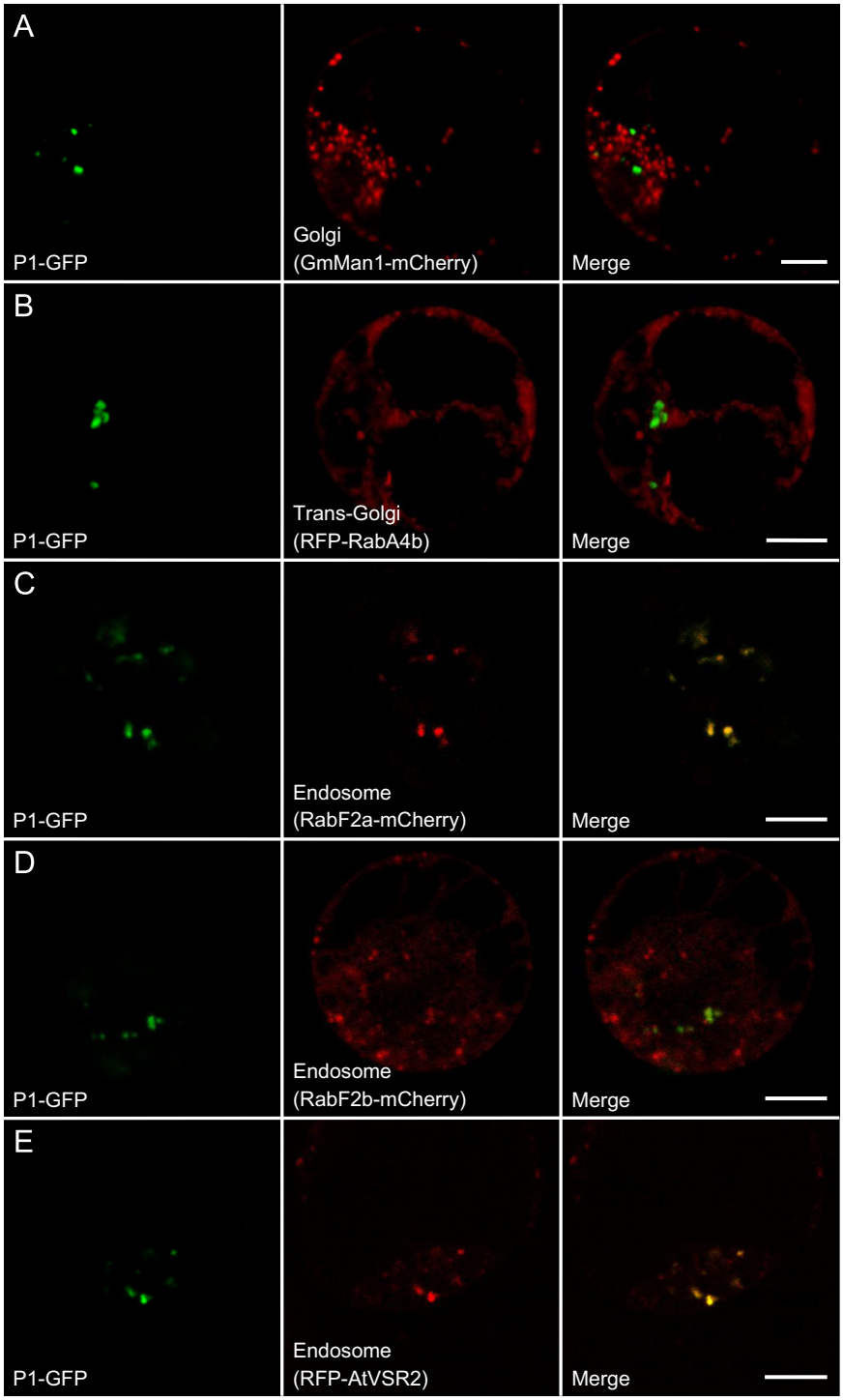

Fig. 4. P1-GFP associates with multivesicular bodies in the endomembrane system. Projection images of arabidopsis protoplasts transfected with pP1-GFP and plasmids that encode proteins localized to the golgi/trans-golgi including: (A) GmMan1-mCherry, (15 optical sections) and (B) RFP-RabA4b, (11 optical sections). Single optical section images of protoplasts transfected with pP1-GFP and plasmids that encode proteins localized to the prevacuolar compartments/multivesicular bodies, including: (C) RabF2a-mCherry, (D) RabF2b-mCherry, and (E) RFP-AtVSR2. Images are labeled with P1-GFP in the green channel or with the labeled host organelle and expressed protein in the red channel. All images were collected at about 20 hpt. Merged images are to the right. Scale bars = 10 μm. (For interpretation of the references to color in this figure legend, the reader is referred to the web version of this article.)

marking the tonoplast, some MVBs, and faintly, the plasma membrane.

To determine whether AMV cDNAs would behave like AMV RNA in the localization of P1-GFP, a mixture of pA2, pA3, and pP1-GFP was used for transfection. In a few protoplasts, P1-GFP accumulated only on MVBs, which suggested that these protoplasts were only expressing P1-GFP. However, about 60% of the remaining fluorescent protoplasts exhibited fluorescence on tonoplasts with or without fluorescent bodies in the cytoplasm as shown in Fig. 6C. Here the tonoplast is marked by both FM4-64 and P1-GFP as are a few MVBs to the right of the tonoplast in the cytoplasm. The remaining 40% of the fluorescent protoplasts accumulated P1-GFP in punctate spots that colocalized with FM4-64 on tonoplasts without overall GFP fluorescence on the

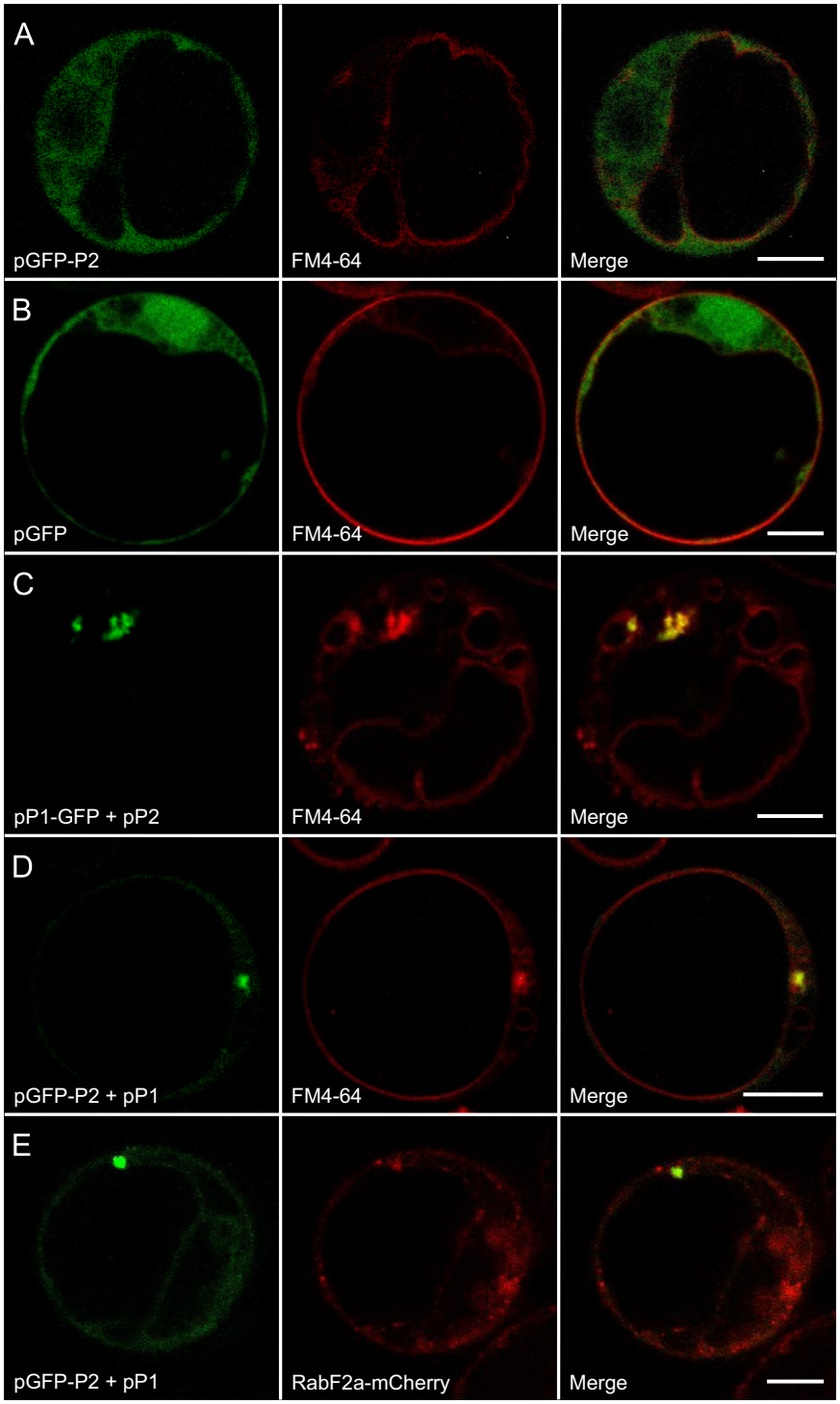

Fig. 5. GFP-P2 accumulates throughout the cytosol when expressed alone and is recruited to multivesicular bodies when expressed with P1. Arabidopsis protoplasts were transfected with (A) pGFP-P2, (B) pGFP, (C) pP1-GFP and pP2, (D) pP1 and pP2-GFP or (E) pGFP-P2, pP1 and RabF2a-mCherry. Samples in panels (A)–(D) were incubated continuously with FM4-64 at 10 μM until imaging: (A) at 28 hpt, (B) at 15 hpt, and (C)–(E) at 20 hpt. All images represent single optical sections (0.44 μm thickness). Images are labeled with the cDNA components used for transfections in the green channel, the tonoplast marker FM4-64, or RabF2a-mCherry in the red channel. Merged images are to the right. Scale bars = 10 μm. (For interpretation of the references to color in this figure legend, the reader is referred to the web version of this article.)

membrane (Fig. 6D). The fluorescence in protoplasts transfected with pP1-GFP and cDNAs (Fig. 6C and D) was generally fainter that in those transfected with pP1-GFP and AMV RNA (Fig. 6A and B). This likely was caused by lower activity of the cDNAs in infection. These results indicate that P1-GFP localized on the tonoplast upon infection following transfection with AMV RNA or the cDNAs, pA2 and pA3, which express full-length RNA1 and RNA2, respectively.

The expression of P2 and full-length RNA enabled P1-GFP to localize on the tonoplast

P1 and P2 GFP-fusion proteins accumulated on MVBs when expressed together; however, P1-GFP accumulated on tonoplasts, as well as, on MVBs upon infection. This suggests that AMV RNA3 or the UTRs of AMV RNA1 and/or 2 are required for P1-GFP distribution on the tonoplast. Therefore, protoplasts were transfected

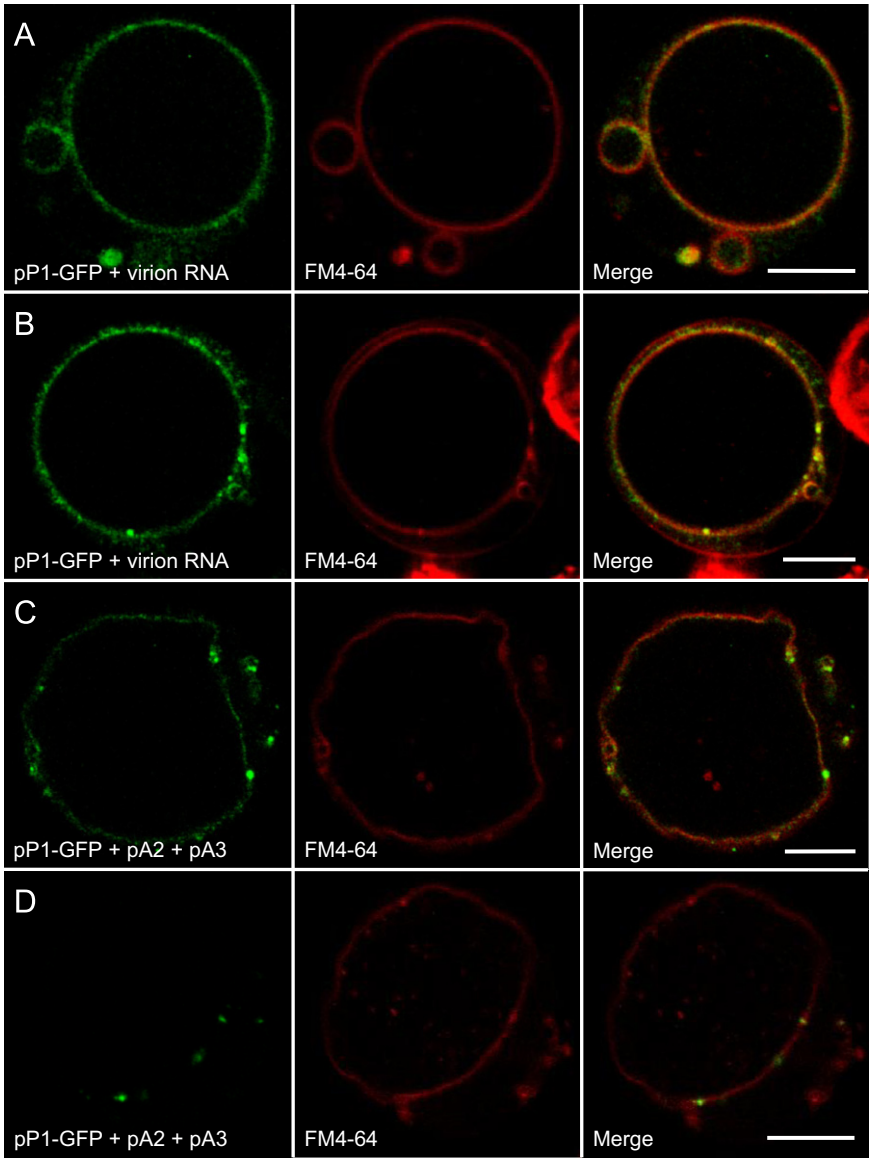

Fig. 6. P1-GFP accumulates on the tonoplast when expressed in presence of AMV RNAs or cDNAs. Images are of single sections of protoplasts transfected with (A) and (B) pP1-GFP and AMV RNA isolated from virions or (C) and (D) pP1-GFP, pA2, and pA3 followed by continuous incubation with FM4-64 at 10 μM until imaging. Images are labeled with the cDNA components used for transfection in the green channel or with the tonoplast marker, FM4-64, in the red channel. All images were collected about 20 hpt. Merged images are to the right. Scale bars = 10 μm. (For interpretation of the references to color in this figure legend, the reader is referred to the web version of this article.)

with pP1-GFP along with individual cDNAs encoding full-length virus RNAs. Following transfection with pP1-GFP and pA1, fluorescent bodies accumulated without tonoplast labeling (Fig. 7A). In this protoplast, the MVBs are between the tonoplast and plasma membrane or in a cytoplasmic strand delimited by tonoplast membranes. Therefore, the presence of RNA1 UTRs did not affect the localization of P1-GFP. Similarly, protoplasts were transfected with pA2 to determine whether the UTRs of RNA 2 along with the expression of the encoded protein, P2, would enable P1-GFP to accumulate on the tonoplast. Fig. 7B shows that pA2 co-expression drove P1-GFP to the tonoplast. The tonoplasts of many protoplasts were fluorescent with or without bright punctate spots although some protoplasts contained only fluorescent spots on the tonoplast with no detectable overall fluorescence. Lastly, protoplasts were transfected with pP1-GFP and pA3, which encodes AMV P3 and CP. Fluorescent bodies of various sizes accumulated. Fig. 7C shows a large fluorescent body that is close to the tonoplast in the cytoplasm. These results indicate that co-expression of full-length RNA1 or RNA3 did not enable P1-GFP to associate with the tonoplast, while the co-expression of A2 resulted in P1-GFP accumulation on the tonoplast. This suggests that P1-GFP and full-length AMV RNA1 or RNA3 is not sufficient and that P2 is also required for tonoplast localization. Therefore, protoplasts were transfected with pP1-GFP, pP2, and pA1 or pA3. P1-GFP accumulated on tonoplasts as overall fluorescence with bright spots (Fig. 7D) or with additional accumulation on bodies in the cytoplasm (Fig. 7E). Therefore, the expression of P1-GFP and full-length RNA1 or RNA3 plus P2 enables the trafficking of P1-GFP to the tonoplast. This suggests that P1, P2, and AMV RNA UTRs are required for tonoplast localization of the replicase complex.

Discussion

AMV cDNA constructs efficiently launch AMV infection in arabidopsis protoplasts (Balasubramaniam et al., 2006); therefore, we designed a system in which the replicase proteins, P1 and P2

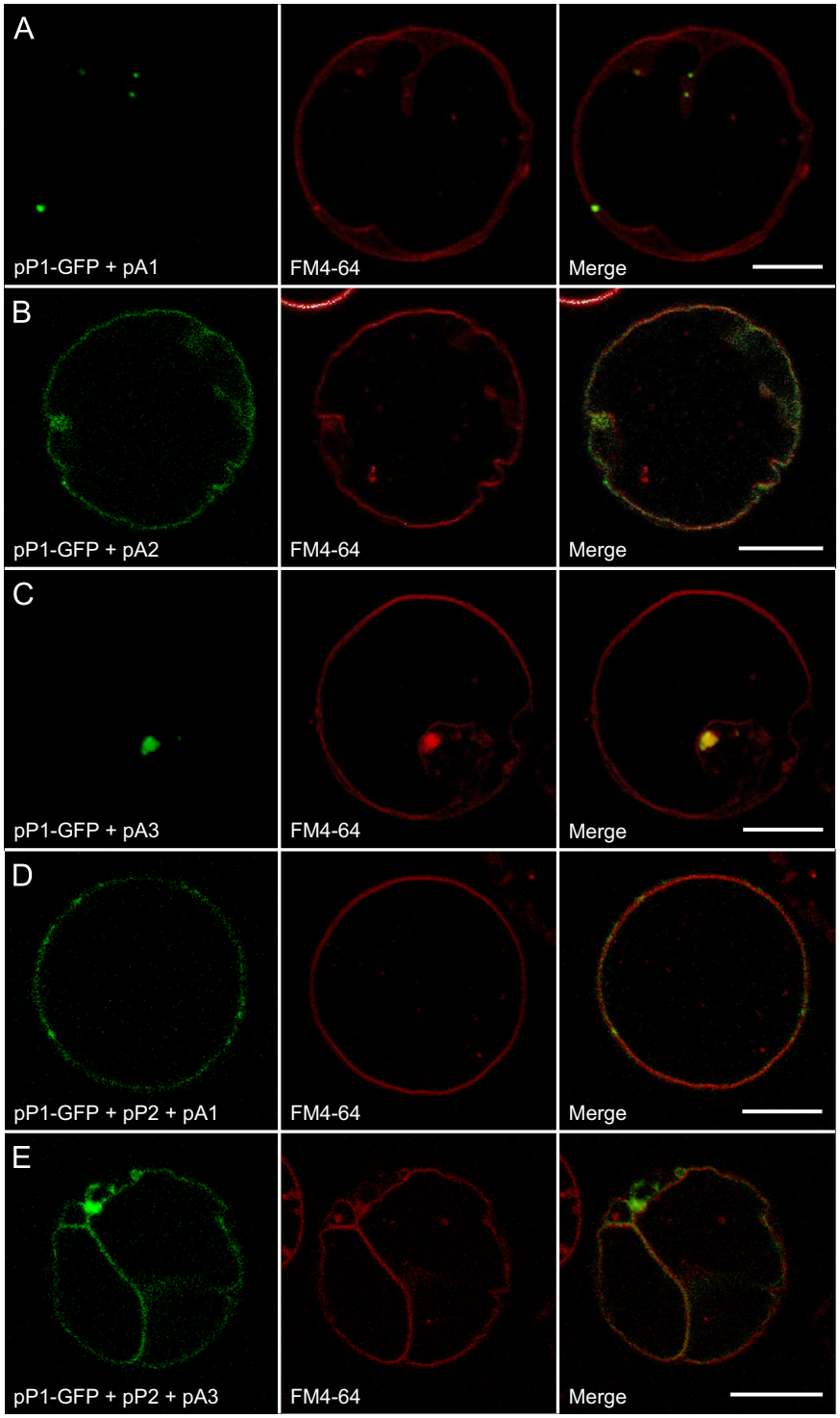

Fig. 7. P1-GFP localizes on the tonoplast in the presence of P2 and a full-length AMV RNA transcript. Images are of single sections of protoplasts transfected with pP1-GFP and (A) pA1, (B) pA2, (C) pA3, or with pP1-GFP, pP2, and (D) pA1, or (E) pA3 followed by continuous incubation with FM4-64 at 10 μM until imaging. Images are labeled with the cDNA components used for transfection in the green channel or with the tonoplast marker, FM4-64, in the red channel. Merged images are to the right. All images were collected about 20 hpt. Scale bars = 10 μm.

or their GFP fusions (Fig. 1) could be tracked in real time to investigate the formation of the replicase complex. The expression of P1-GFP protein was robust soon after transfection of arabidopsis protoplasts. It accumulated as small punctate spots and large globular-shaped bodies, both of which increased in number and size with time. All bodies colocalized with the endocytic marker, FM4-64, which associates with various endosomes, multivesicular bodies, Golgi, the trans-Golgi network and, ultimately, the tonoplast (Bolte et al., 2004). P1-GFP's association with FM4-64 and its lack of association with chloroplasts, Golgi, and peroxisomes suggested that it accumulated in the endosomal compartment. This was confirmed by colocalization

with MVB-specific proteins including: RabF2a-mCherry, RabF2b-mCherry, and RFP-AtVSR2 (Ueda et al., 2001; Sohn et al., 2003; Tse et al., 2004; Miao et al., 2006). RabF2a also referred to as Rha1 and RabF2b also referred to as Ara7 are two of more than 50 members of the Rab family of GTPases in arabidopsis, which have roles in vesicle-mediated transport as do all Rab proteins (Marcote et al., 2000). The Rab proteins interact with various other proteins to cycle between a cytosolic GDP-bound inactive state and membrane associated GTP-bound active state and with downstream effector proteins to regulate budding, movement, and fusion of vesicles with membranes (Pfeffer and Aivazian, 2004; Saito and Ueda, 2009). RabF2a and RabF2b are members of the RabF subfamily in plants that have roles in endosomal trafficking of soluble proteins to the vacuole (Sohn et al., 2003; Lee et al., 2004; Haas et al., 2007). Rab proteins have been found to be associated with the entry, trafficking, and replication of a number of viruses. For example, mammalian Rab1 and Rab5, which are homologues of arabidopsis Rab1b (Batoko et al., 2000) and RabF2a (Sohn et al., 2003), respectively, are required for efficient replication of HCV (Stone et al., 2007; Manna et al., 2010). In addition, the Rab1 GTPase-activating protein, TBC1D20, directly interacts with the HCV nonstructural protein, NS5A, for efficient replication (Sklan et al., 2007a, 2007b). Early endosomes containing Rab5 are involved in the trafficking of SFV to late endosomes containing Rab7 (Vonderheit and Helenius, 2005). And recently, the RabGDP dissociation inhibitor (GD12) of *Nicotiana benthamiana* was shown to interact with the 126 kDa replication protein of TMV to relocate GD12 from the cytoplasm to sites in the ER where infection is established (Kramer et al., 2011).

Coexpression of P2 with P1-GFP did not affect the localization of P1-GFP. This finding along with localization studies of P1-GFP expression alone, indicated that P1-GFP did not associate with the tonoplast, the proposed site of AMV replication (Van Der Heijden et al., 2001), but rather accumulated as P1/P2 complexes in the endocytic pathway. This is in contrast to the behavior of other viral nonstructural proteins similar to P1 encoded by other members of the *Bromoviridae*. For example, the 1a protein of BMV (Restrepo-Hartwig and Ahlquist, 1996, 1999; den Boon et al., 2001) and of CMV (Cillo et al., 2002, Kim et al., 2006) independently localize to ER membranes and tonoplasts, respectively, where replication takes place. Likewise, homologous proteins of the following viruses localize to sites of replication when expressed alone: the 126K protein of TMV localizes to the ER (dos Reis Figueira et al., 2002), the 140K protein of TYMV localizes to chloroplast membranes (Prod'homme et al., 2003), and the P33 protein of TBSV localizes to peroxisome membranes (McCartney et al., 2005).

The AMV P2 protein, which is the putative RNA polymerase, accumulated throughout the cytosol when expressed alone suggesting that it contains no targeting information. Its behavior is similar to that of other viral polymerase proteins such as the 2a protein of BMV (Chen and Ahlquist, 2000) and the 66K protein of TYMV (Prod'homme et al., 2003). In the presence of P1, however, GFP-P2 was found to colocalize with RabF2a-Cherry-tagged MVBs. The recruitment of GFP-P2 to the MVBs is likely mediated through its interaction with P1, which has been shown to occur in vitro and in yeast (Reichert et al., 2007; Van Der Heijden et al., 2001). Therefore, AMV is similar to other viruses in that the polymerase is recruited to sites of replication by another viral nonstructural protein. The BMV 1a protein recruits the 2a polymerase protein from the cytoplasm to the ER membrane (Chen and Ahlquist, 2000). The p33 protein of *Cucumber necrosis virus* recruits the p92 polymerase protein to peroxisomal membranes (Panavas et al., 2005) and the TYMV 104K protein brings the 66K protein to the chloroplast membrane (Jakubiec et al., 2004; Prod'homme et al., 2003).

In contrast to its localization when expressed alone and with P2, P1-GFP appeared on tonoplasts when expressed in infected protoplasts. This confirms that the tonoplast is the site where AMV replicase proteins ultimately accumulate and it is likely the site of replication. The presence of P1-GFP on a few MVBs in infected cells is intriguing and raises the possibility that AMV replication may start on the MVBs and progress to the tonoplast or that AMV can replicate on both MVB membranes and the tonoplast. Recently, the replicase complex of two alphaviruses, SFV and *Sindbis virus*, was described as trafficking between the plasma membrane and cytopathic vacuoles. Both of these viruses were thought to form replication complex spherules only on cytopathic vacuoles made up of lysosomes and modified endosomes, which are equivalent to plant vacuoles and MVBs (Froshauer et al., 1988; Jiang and Rogers, 1998; Salonen et al., 2003; Vonderheit and Helenius, 2005; Mo et al., 2006). However, live-cell imaging and electron microscopy indicated that the replication complexes form at the plasma membrane and are relocated to the cytopathic vacuoles (Spuul et al., 2010; Frolova et al., 2010). The components for replication of other viruses have been reported to come together on distinct organelles and traffic to other sites for replication. For example, small vesicles concentrate the proteins and RNAs for replication of *Turnip mosaic* potyvirus at the ER and transport them to the chloroplasts for replication (Wei et al., 2010).

To sort out the components required for tonoplast localization, P1-GFP was expressed with P2 and different AMV cDNAs. Tonoplast targeting occurred following transfection with mixtures containing pP1-GFP plus A2 or pP1-GFP, pP2 and A1, or A3. These results indicate that P1-GFP targeting to the tonoplast is dependent on the presence of P2 and 3′ and/or 5′ UTRs of an AMV RNA. Our data add to the results of Vlot et al. (2001), who reported that an active AMV replicase could only be isolated from plants transiently expressing full-length RNA1 and 2, whereas it could not be isolated if the RNAs lacked 3′UTRs. Thus, a 3′UTR was required for the formation of an active replicase complex. These results and ours suggest that the formation of an active AMV complex is required for localization on the tonoplast. Recently, the formation of replication complex of *Flock house* nodavirus (FHV) was found to require the presence of a replication competent FHV RNA as well as the FHV polymerase (Kopek et al., 2010). Thus, spherule formation of FHV requires RNA synthesis. Our results indicate that, of the AMV proteins involved in replication, only P1 has affinity for membranes. Therefore, our results suggest that that P1 orchestrates the assembly of the AMV replicase complexes by recruiting P2 and AMV RNAs to MVBs, which transport the complexes to the tonoplast.

Materials and methods

Plasmids

All PCR reactions were performed using *pfu* DNA polymerase for enhanced fidelity and production of blunt ended PCR products. The PCR products in all final vectors were sequenced for confirmation. A linear DNA, p35S, containing the 35S promoter for expression of P1, P2, GFP, and GFP fusions was made by digesting psmRSGFP (Davis and Vierstra, 1998) with BamHI, filling in the ends using Klenow DNA polymerase, and digesting with SacI to remove the resident GFP ORF sequence. To make the vector for expression of GFP, pGFP, the ORF for the enhanced GFP (EGFP) from the pEGAD vector (Cutler et al., 2000) was amplified using the forward primer, GFP-BamHI, to add a BamHI site just before the start codon of the EGFP ORF and the reverse primer, GFP-SacI, to add a SacI site and a stop codon to the end of the EGFP ORF.

Table 1
Sequences of oligonucleotides used in this study[a].

Oligonucleotide	Sequence (5′–3′)
P1-F-SmaI	**TATCCCGGG**ATGAATGCTGACG
A1-BsiWI	CGGACGTACGACTTTAGAGAC
A1-NcoI	CCCATGCCATGGATTAGTTG
P1-R-SacI	**CCCACGAGCTC**TCAGAAATTAGTATTATAG
P2-F-SmaI	**TATCCCGGG**ATGTTCACTCTTTTGA
P2-R-BamHI	CATTGGAATGATGGATCCACTGA
P2-F-KpnI	GTCCTGCCGGTACCGAATCCA
P2-R-SacI	**TATTTGAGCTC**TCAAGCTCGGCGT
GFP-BamHI	**TTAAGGATCC**GGTCGCCACCATG
GFP-SacI	**ACCAGAGCTC**TTACTTGTACAGCTCGTC
P1-BglII	CCAGAGTACTGGGATCTATCGAAG
P1-Ala10-SacI-XhoI	**CGTTTGAGCTCAATAATCTCGAG**GGCCGCTGCCGCAGCGGCAGCGGCCGCAGCGAAATTAGTATTATAGCT
GFP-XhoI	**GCATATCTCGAG**ATGGTGAGCAAG
GFP-SacI	**ACCAGAGCTC**TTACTTGTACAGCTCGTC

[a] Underlined sequences in bold are added restriction enzyme sites, which are indicated in the corresponding oligonucleotide name. Sequences in bold without underlining are nucleotides added for cloning while sequences in regular type correspond to AMV RNA sequences.

(Table 1 lists the primer sequences used in this study). The PCR product was digested with BamHI and SacI, ligated to p35S.

cDNAs of RNA1 and 2 had been previously cloned into the pSP64 and pUC19 vectors under control of the T7 promoter to make pA1-pSP64 and pA2-pUC19, respectively. The infectivity of the in vitro RNA transcripts from these vectors had been confirmed previously (Balasubramaniam et al., 2006). The 5′ and 3′ ends of the ORFs of RNA1 and 2 in pA1-pSP64 and pA2-pUC19, respectively, were amplified by PCR and the products were used to replace the 5′ and 3′ UTR sequences in pA1-pSP64 and pA2-pUC19. The resulting plasmids, pP1-pSP64 and pP2-pUC19 contained only the ORFs of P1 and P2, respectively. Thus, to amplify the 5′ end of the P1 ORF, we used the forward primer, P1-F-SmaI, which added a SmaI site just before the start codon of the P1 ORF, and the reverse primer, A1-BsiWI, which spans the unique BsiWI restriction site of the cDNA of RNA1. The PCR product was digested with BsiWI and ligated to pA1-pSP64, which had been digested with BamHI, filled in, and then digested with BsiWI, to produce pA1Δ5′UTR-pSP64. The 3′ end of the P1 ORF was amplified using the forward primer, A1-NcoI, which spans the unique NcoI restriction site of the cDNA of RNA1, and the reverse primer, P1-R-SacI, which added a SacI site next to the P1 ORF stop codon. The PCR product was digested with NcoI and SacI and ligated to pA1Δ5′UTR-pSP64, which had been digested with the same restriction enzymes, to produce pP1-pSP64. To amplify the 5′ end of the P2 ORF, we used the forward primer, P2-F-SmaI, which added a SmaI site just before the P2 ORF start codon, and the reverse primer, P2-R-BamHI, which spans the unique BamHI restriction site of the cDNA of RNA2. The PCR product was digested with BamHI and ligated to pA2-pUC19, which had been digested with PstI, filled in, and then digested with BamHI, to produce pA2Δ5′UTR-pUC19. The 3′ end of the P2 ORF was amplified using the forward primer, P2-F-KpnI, which spans the unique KpnI restriction site of the cDNA of RNA2, and the reverse primer, P2-R-SacI, which added a SacI site next to the P2 ORF stop codon. The PCR product was digested with KpnI and SacI and ligated to pA2Δ5′UTR-pUC19, which had been digested with the same restriction enzymes, to produce pP2-pUC19.

The EGFP ORF obtained from the pEGAD vector (Cutler et al., 2000) was fused to P1 and P2 to make GFP-P1, P1-GFP and GFP-P2 expression vectors. Thus, the EGFP ORF followed by 10 Ala codons and restriction enzyme sites (EcoRI, SmaI, Hind III, and BamHI) was subcloned from the pEGAD vector to the Litmus 28 vector (New England Biolabs) using double digestion with AgeI and BamHI to make pGFP-Ala(10)-L28. Then, the EGFP ORF followed by the 10 Ala codons was released as a blunt-ended fragment from pGFP-Ala(10)-L28 using StuI and SmaI digestion, followed by ligation to SmaI digested pP1-pSP64 and pP2-pUC19, to produce pGFP-Ala(10)-P1-pSP64 and pGFP-Ala(10)-P2-pUC19, respectively. The GFP-Ala(10)-P1 sequence was released from pGFP-Ala(10)-P1-pSP64 by digestion with HindIII, followed by filling the ends with klenow DNA polymerase, and finally, digestion with SacI. The GFP-Ala(10)-P1 sequence was then ligated to the linear p35S vector to make pGFP-P1. Similarly, GFP-Ala(10)-P2 was released from pGFP-Ala(10)-P2-pUC19 by digestion with XbaI, followed by filling the ends with klenow DNA polymerase, and finally, digestion with SacI. The GFP-Ala(10)-P2 sequence was then ligated to the linear p35S to make pGFP-P2. To make vectors for the expression of wild-type P1 and P2, the P1 and P2 ORFs sequences were removed from pGFP-P1 and pGFP-P2, respectively, by digestion with SmaI and SacI, followed by ligation to the linear p35S vector to make pP1 and pP2. To make pP1-GFP expression vector, the 3′ end of the P1 ORF was amplified using the forward primer, P1-BglII, which spans the unique BglII restriction site of the cDNA of RNA1, and the reverse primer, P1-Ala10-SacI-XhoI, which added SacI and XhoI restriction sites and 10 Ala codons, as well as removing the P1 ORF stop codon. The PCR product was digested with BglII and XhoI and ligated to pP1, which had been digested with the same restriction enzymes, to produce pP1-Ala(10). The EGFP ORF from the pEGAD vector (8) was amplified using the forward primer, GFP-XhoI, which added an XhoI restriction site before the EGFP ORF start codon, and the reverse primer, GFP-SacI, which added a SacI restriction site next to EGFP stop codon. The PCR product was digested with XhoI and SacI and ligated to pP1-Ala(10), which had been digested with the same restriction enzymes, to make pP1-GFP.

The plasmids, px-rk, ER-ck, and G-rk (Nelson et al., 2007), pRabF2a-mCherry, and pRabF2b-mCherry were obtained from the Arabidopsis Stock Center. The plasmids, pmRFP-AtVSR2 (Miao et al., 2006) and pRFP-RabA4b (Preuss et al., 2004) were kindly provided by Dr. Liwen Jiang and Dr. Stanton Gelvin, respectively.

Isolation of arabidopsis protoplasts

Protoplasts were isolated from an *Arabidopsis thaliana* cell culture that was maintained as previously described (Delgado et al., 1998). The isolation of protoplasts was as previously

described (Ueda et al., 2001) with slight modifications. Briefly, cells were digested in an enzyme mixture containing 2% cellulysin (Calbiochem), 0.1% pectolyaseY-23 (Seishin Pharmaceutical), and 400 mM mannitol for 90 min at 30 °C with gentle shaking followed by centrifugation at 50 × *g* for 2 min to collect protoplasts, which were then resuspended in mannitol/$CaCl_2$ solution (400 mM mannitol and 70 mM $CaCl_2$). Viable protoplasts were isolated by sedimentation at 50 × *g* for 10 min onto a cushion of 20% sucrose solution, washed with mannitol/$CaCl_2$ solution twice, pelleted, and resuspended in mannitol/$MgCl_2$ solution (400 mM mannitol, 15 mM $MgCl_2$, and 5 mM MES, pH 5.7) (Negrutiu et al., 1987) at a concentration 10^6 protoplasts/ml.

Transfection and immunofluorescent assay of protoplasts

Protoplast transfection was as described (Ueda et al., 2001) with slight modification. Briefly, 100 μl of a protoplast suspension at 10^6 protoplasts/ml were added to 5 μg of each plasmid DNA and 10–30 μg of sheared salmon sperm carrier DNA, or for cotransfections with RNA and cDNA, to 15 μg of cDNA, 5 μg of AMV RNA, which had been isolated by phenol extraction and ethanol precipitation from virions, and 15 μg of carrier DNA. The suspension was briefly mixed and 400 μl of a PEG solution (40% PEG 4000, 100 mM $Ca(NO_3)_2$, and 400 mM mannitol) were added. The samples were kept on ice for 20 min followed by gentle dilution with 2.5 ml of solution containing 400 mM mannitol, 125 mM $CaCl_2$, 5 mM KCl, 5 mM glucose and 1.5 mM MES pH 5.7. The protoplasts were collected by centrifugation at 50 × *g* for 7 min, washed once with 400 mM mannitol, and resuspended in 0.5 ml culture medium (1 × Gamborg's B-5 medium, 100 mM glucose, and 400 mM mannitol). To mark organelles in the endocytic pathway (Bolte et al., 2004; Griffing, 2008; Van Gisbergen et al., 2008), FM4-64 dye (Invitrogen) was added at 10 μM to the culture medium for continuous labeling until observation in the confocal microscope. An immunofluorescent assay for AMV CP was used to determine the percentage of infected protoplasts as previously described (Otsuki and Takebe, 1969). Briefly, protoplasts were spotted onto glass slides coated with Mayer's albumin, quickly dried, and fixed in acetone. Polyclonal CP antiserum prepared in rabbits and anti-rabbit IgG conjugated with fluorescein isothiocyanate (Sigma) were used to detect AMV CP.

In vitro translation and protein analysis

AMV RNA isolated from virions was translated in vitro using wheat germ extract (Promega) as described by the manufacturer. To analyze protein accumulation during infection, protoplasts were collected by centrifugation, resuspended in an equal volume of 2 × electrophoresis sample buffer (100 mM Tris–Cl, pH 6.8, 4% SDS, 0.2% bromophenol blue, 20% glycerol, 2% β-mercaptoethanol), and boiled for 5–10 min. Proteins were separated in 10 or 12% SDS-polyacrylamide gels by electrophoresis and transferred to PVDF membranes for western analysis using standard procedures (Sambrook and Russell, 2001). Polyclonal rabbit antiserum was used to detect the CP followed by alkaline phosphatase-conjugated anti-rabbit IgG.

Confocal microscopy

Protoplasts expressing fluorescent proteins and/or FM4-64 were observed using Zeiss laser scanning confocal microscopes (LSM 510, 610, and 710). The 488 nm excitation line with a 505–530 nm band pass emission filter was used to detect GFP and the 543 nm excitation line with a 560–615 nm band pass emission filter was used to detect FM4-64, mRFP, and mCherry. Alternatively, the emission of FM4-64 was detected at 593–647 nm using spectral scanning with the Meta detector. Chloroplast autofluorescence was imaged using the 488 nm laser line for excitation and the 615 nm long pass emission filter for detection. For experiments involving two or more fluorescent markers, images were collected sequentially to avoid channel bleed through. Zen (Zeiss), Imaris (Bitplane), and Photoshop CS3 (Adobe) software were used for post processing of all images.

Acknowledgments

We thank Dr. Nicholas C. Carpita and Anna Olek for the arabidopsis suspension cell culture and help with its culture, Dr. Stanton Gelvin for the Trans-Golgi marker, RFP-RabA4b, Dr. Lliwen Jiang for mRFP-AtVSR2, and Dr. Daniel Szymanski for the psmRSGFP vector. We also thank Dr. Angus Murphy and Dr. Wendy Peer for assistance with the confocal microscope and Omayra Mendez for assistance with transfection and imaging of protoplasts.

References

Alblas, F., Bol, J.F., 1978. Coat protein is required for infection of cowpea protoplasts with Alfalfa mosaic virus. J. Gen Viol. 14, 653–656.

Balasubramaniam, M., Ibrahim, A., Kim, B.-S., Loesch-Fries, L.S., 2006. *Arabidopsis thaliana* is an asymptomatic host of *Alfalfa mosaic virus*. Virus Res. 121, 215–219.

Batoko, H., Zheng, H.-Q., Hawes, C., Moore, I., 2000. A Rab1 GTPase is required for transport between the endoplasmic reticulum and Golgi apparatus and for normal Golgi movement in plants. The Plant Cell 12, 2201–2217.

Bolte, S., Talbot, C., Boutte, Y., Catrice, O., Read, N.D., Satiat-Jeunemaitre, B., 2004. FM-dyes as experimental probes for dissecting vesicle trafficking in living plant cells. J. Microsc. 214, 159–173.

Carette, J.E., Stuiver, M., Van Lent, J., Wellink, J., Van Kammen, A., 2000. Cowpea mosaic virus infection induces a massive proliferation of endoplasmic reticulum but not Golgi membranes and is dependent on de novo membrane synthesis. J. Virol. 74, 6556–6563.

Chen, J., Ahlquist, P., 2000. Brome mosaic virus polymerase-like protein 2a is directed to the endoplasmic reticulum by helicase-like viral protein 1a. J. Virol. 74, 4310–4318.

Cillo, F., Roberts, I.M., Palukaitis, P., 2002. In situ localization and tissue distribution of the replication-associated proteins of *Cucumber mosaic virus* in tobacco and cucumber. J. Virol. 76, 10654–10664.

Cutler, S.R., Ehrhardt, D.W., Griffitts, J.S., Somerville, C.R., 2000. Random GFP::cDNA fusions enable visualization of subcellular structures in cells of *Arabidopsis* at a high frequency. Proc. Nat. Acad. Sci. U.S.A. 97, 3718–3723.

Davis, S.J., Vierstra, R.D., 1998. Soluble, highly fluorescent variants of green fluorescent protein (GFP) for use in higher plants. Plant Mol. Biol. 36, 521–528.

Delgado, I.J., Wang, Z., de Rocher, A., Keegstra, K., Raikhel, N.V., 1998. Cloning and characterization of *AtRGP1*-A reversibly autoglycosylated Arabidopsis protein implicated in cell wall biosynthesis. Plant Physiol. 116, 1339–1349.

den Boon, J.A., Chen, J., Ahlquist, P., 2001. Identification of sequences in Brome mosaic virus replicase protein 1a that mediate association with endoplasmic reticulum membranes. J. Virol. 75, 12370–12381.

den Boon, J.A., Ahlquist, P., 2010. Organelle-like membrane compartmentalization of positive-strand RNA virus replication factories. Ann. Rev. Microbiol. 64, 241–256.

Diaz, A., Wang, X., Ahlquist, P., 2010. Membrane-shaping host reticulon proteins play crucial roles in viral RNA replication compartment formation and function. Proc. Nat. Acad. Sci. U.S.A. 107, 16291–16296.

dos Reis Figueira, A., Golem, S., Goregaoker, S.P., Culver, J.N., 2002. A nuclear localization signal and a membrane association domain contribute to the cellular localization of the Tobacco mosaic virus 126-kDa replicase protein. Virology 301, 81–89.

Egger, D., Wölk, B., Gosert, R., Bianchi, L., Blum, H.E., Moradpour, D., Bienz, K., 2002. Expression of Hepatitis C virus proteins induces distinct membrane alterations including a candidate viral replication complex. J. Virol. 76, 5974–5984.

Frolova, E.I., Gorchakov, R., Pereboeva, L., Atasheva, S., Frolov, I., 2010. Functional Sindbis virus replicative complexes are formed at the plasma membrane. J. Virol. 84 (22), 11679–11695.

Froshauer, S., Kartenbeck, J., Helenius, A., 1988. Alphavirus RNA replicase is located on the cytoplasmic surface of endosomes and lysosomes. J. Cell Biol. 107, 2075–2086.

Gonsalves, D., Garnsey, S.M., 1975. Infectivity of heterologous RNA-protein mixtures from Alfalfa mosaic, Citrus leaf rugose, Citrus variegation, and Tobacco streak viruses. Virology 67, 319–326.

Gomord, V., Denmat, L.-A., Fitchette-Laine, A.-C., Satiat-Jeunemaitre, B., Hawes, C., Faye, L., 1997. The C-terminal HDEL sequence is sufficient for retention of

secretory proteins in the endoplasmic reticulum (ER) but promotes vacuolar targeting of proteins that escape the ER. The Plant J. 11, 313–325.
Gosert, R., Egger, D., Lohmann, V., Bartenschlager, R., Blum, H.E., Bienz, K., Moradpour, D., 2003. Identification of the Hepatitis C virus RNA replication complex in Huh-7 cells harboring subgenomic replicons. J. Virol. 77, 5487–5492.
Griffing, L.R., 2008. FRET analysis of transmembrane flipping of FM4-64 in plant cells: is FM4-64 a robust marker for endocytosis? J. Microsc. 231, 291–298.
Guogas, L.M., Filman, D.J., Hogle, J.M., Gehrke, L., 2004. Cofolding organizes Alfalfa mosaic virus RNA and coat protein for replication. Science 306, 2108–2111.
Haas, T.J., Sliwinski, M.K., Martínez, D.E., Preuss, M., Ebine, K., Ueda, T., Nielsen, E., Odorizzi, G., Otegui, M.S., 2007. The *Arabidopsis* AAA ATPase SKD1 is involved in multivesicular endosome function and interacts with its positive regulator LYST-INTERACTING PROTEIN5. The Plant Cell 19, 1295–1312.
Hatta, T., Bullivant, S., Matthews, R.E.F., 1973. Fine structure of vesicles induced in chloroplasts of Chinese cabbage leaves by infection with Turnip yellow mosaic virus. J. Gen. Virol. 20, 37–50.
Hatta, T., Francki, R.I.B., 1981. Cytopathic structures associated with tonoplasts of plant-cells infected with Cucumber mosaic and Tomato aspermy viruses. J. Gen. Virol. 53, 343–346.
He, Z.-H., Cheeseman, I., He, D., Kohorn, B.D., 1999. A cluster of five cell wall-associated receptor kinase genes, *Wak1–5*, are expressed in specific organs of *Arabidopsis*. Plant Mol. Biol. 39, 1189–1196.
Heinlein, M., Padgett, H.S., Gens, J.S., Pickard, B.G., Casper, S.J., Epel, B.L., Beachy, R.N., 1998. Changing patterns of localization of the Tobacco mosaic virus movement protein and replicase to the endoplasmic reticulum and microtubules during infection. The Plant Cell 10, 1107–1120.
Jakubiec, A., Notaise, J., Tournier, V., Héricourt, F., Block, M.A., Drugeon, G., van Aelst, L., Jupin, I., 2004. Assembly of *Turnip yellow mosaic virus* replication complexes: interaction between the proteinase and polymerase domains of the replication proteins. J. Virol. 78, 7945–7957.
Jiang, L.W., Rogers, J.C., 1998. Integral membrane protein sorting to vacuoles in plant cells: evidence for two pathways. J. Cell Biol. 143, 1183–1199.
Kim, M.J., Kim, H.R., Peak, K.-H., 2006. *Arabidopsis* tonoplast proteins TIP1 and TIP2 interact with the Cucumber mosaic virus 1a replication protein. J. Gen. Virol. 87, 3425–3431.
Kopek, B.G., Settles, E.W., Friesen, P.D., Ahlquist, P., 2010. Nodavirus-induced membrane rearrangement in replication complex assembly requires replicase protein A, RNA templates, and polymerase activity. J. Virol. 84 (24), 12492–12503.
Krab, I.M., Caldwell, C., Gallie, D.R., Bol, J.F., 2005. Coat protein enhances translational efficiency of *Alfalfa mosaic virus* RNAs and interacts with the eIF4G component of initiation factor eIF4F. J. Gen. Virol. 86, 1841–1849.
Kramer, S.R., Goregaoker, S.P., Culver, J.N., 2011. Association of the *Tobacco mosaic virus*126 kDa replication protein with a GDI protein affects host susceptibility. Virology 414, 110–118.
Kujala, P., Ahola, T., Ehsani, N., Auvinen, P., Vihinen, H., Kääriäinen, L., 1999. Intracellular distribution of Rubella virus nonstructural protein P150. J. Virol. 73, 7805–7811.
Lam, S.K., Tse, Y.C., Miao, Y., Li, H.-Y., Wang, J., Lo, S.W., Jiang, L., 2007. Molecular characterization of plant prevacuolar and endosomal compartments. J. Integr. Plant Biol. 49, 1119–1128.
Lee, G.-J., Sohn, E.J., Lee, M.H., Hwang, I., 2004. The *Arabidopsis* Rab5 homologs Rha1 and Ara7 localize to the prevacuolar compartment. Plant Cell Physiol. 45, 1211–1220.
Magliano, D., Marshall, J.A., Bowden, D.S., Vardaxis, N., Meanger, J., Lee, J.-Y., 1998. Rubella virus replication complexes are virus-modified lysosomes. Virology 240, 57–63.
Manna, D., Aligo, J., Xu, C., Park, W.S., Koc, H., Heo, W.D., Konan, K.V., 2010. Endocytic Rab proteins are required for hepatitis C virus replication complex formation. Virology 398, 21–37.
Marcote, M.J., Gu, F., Gruenberg, J., Aniento, F., 2000. Membrane transport in the endocytic pathway: animal versus plant cells. Protoplasma 210, 123–132.
Más, P., Beachy, R.N., 1999. Replication of Tobacco mosaic virus on endoplasmic reticulum and role of the cytoskeleton and virus movement protein in intracellular distribution of viral RNA. J. Cell Biol. 147, 945–958.
McCartney, A.W., Greenwood, J.S., Fabian, M.R., White, K.A., Mullen, R.T., 2005. Localization of the tomato bushy stunt virus replication protein p33 reveals a peroxisome-to-endoplasmic reticulum sorting pathway. The Plant Cell. 17, 3513–3531.
Miao, Y., Yan, P.K., Kim, H., Hwang, I., Jiang, L., 2006. Localization of green fluorescent protein fusions with the seven arabidopsis vacuolar sorting receptors to prevacuolar compartments in tobacco BY-2 cells. Plant Physiol. 142, 945–962.
Miao, Y., Li, K.Y., Li, H.-Y., Yao, X., Jiang, L., 2008. The vacuolar transport of aleurain-GFP and 2S albumin-GFP fusions is mediated by the same pre-vacuolar compartments in tobacco BY-2 and Arabidopsis suspension cultured cells. The Plant J. 56, 824–839.
Miller, D.J., Schwartz, M.D., Ahlquist, P., 2001. Flock house virus RNA replicates on outer mitochondrial membranes in *Drosophila* cells. J. Virol. 75, 11664–11676.
Mo, B.X., Tse, Y.C., Jiang, L.W., 2006. Plant prevacuolar/endosomal compartments. Int. Rev. Cytol. 253, 95–125.
Nagy, P.D., Pogany, J., 2012. The dependence of viral RNA replication on co-opted host factors. Nat. Rev. Microbiol. 10, 137–149.
Neeleman, L., Olsthoorn, R.C.L., Linthorst, H.J.M., Bol, J.F., 2001. Translation of a nonpolyadenylated viral RNA is enhanced by binding of viral coat protein or polyadenylation of the RNA. Proc. Nat. Acad. Sci. U.S.A. 98, 14286–14291.
Negrutiu, I., Shillito, R., Potrykus, I., Biasini, G., Sala, F., 1987. Hybrid genes in the analysis of transformation conditions. 1. Setting up a simple method for direct gene-transfer in plant protoplasts. Plant Mol. Biol. 8, 363–373.
Nelson, B.K., Cai, X., Nebenfuhr, A., 2007. A multicolored set of in vivo organelle markers for co-localization studies in Arabidopsis and other plants. The Plant J. 51, 1126–1136.
Otsuki, Y., Takebe, I., 1969. Fluorescent antibody staining of Tobacco mosaic virus antigen in tobacco mesophyll protoplasts. Virology 38, 497–499.
Panavas, T., Hawkins, C.M., Panaviene, Z., Nagy, P.D., 2005. The role of the p33:p33/p92 interaction domain in RNA replication and intracellular localization of p33 and p92 proteins of *Cucumber necrosis* tombusvirus. Virology 338, 81–95.
Pfeffer, S., Aivazian, D., 2004. Targeting Rab GTPases to distinct membrane compartments. Nat. Rev. Mol. Cell Biol. 5, 886–896.
Preuss, M.L., Serna, J., Falbel, T.G., Bednarek, S.Y., Nielsen, E., 2004. The Arabidopsis Rab GTPase RabA4b localizes to the tips of growing root hair cells. The Plant Cell 16, 1589–1603.
Prod'homme, D., Jakubiec, A., Tournier, V., Drugeon, G., Jupin, I., 2003. Targeting of the *Turnip yellow mosaic virus* 66K replication protein to the chloroplast envelope is mediated by the 140K protein. J. Virol. 77, 9124–9135.
Record, R.D., Griffing, L.R., 1988. Convergence of the endocytic and lysosomal pathways in soybean protoplasts. Plants 176, 425–432.
Reichert, V.L., Choi, M., Petrillo, J.E., Gehrke, L., 2007. Alfalfa mosaic virus coat protein bridges RNA and RNA-dependent RNA polymerase in vitro. Virology 364, 214–226.
Restrepo-Hartwig, M.A., Ahlquist, P., 1996. Brome mosaic virus helicase- and polymerase-like proteins colocalize on the endoplasmic reticulum at sites of viral RNA synthesis. J. Virol. 70, 8908–8916.
Restrepo-Hartwig, M., Ahlquist, P., 1999. Brome mosaic virus RNA replication proteins 1a and 2a colocalize and 1a independently localizes on the yeast endoplasmic reticulum. J. Virol. 73, 10303–10309.
Saint-Jore-Dupas, C., Gomord, V., Paris, N., 2004. Protein localization in the plant Golgi apparatus and the *trans*-Golgi network. Cell. Mol. Life Sci. 61, 159–171.
Saito, C., Ueda., T., 2009. Functions of RAB and SNARE proteins in plant life. Int. Rev. Cell and Mol. Biol. 274, 183–233.
Salonen, A., Vasiljeva, L., Merits, A., Magden, J., Jokitalo, E., Kääriäinen, L., 2003. Properly folded nonstructural polyprotein directs the Semliki Forest virus replication complex to the endosomal compartment. J. Virol. 77, 1691–1702.
Sambrook, J., Russell, D.W., 2001. Molecular Cloning, a Laboratory Manual, third ed. Cold Spring Harbor Laboratory Press, Cold Spring Harbor, New York.
Schwartz, M., Chen, J., Janda, M., Sullivan, M., den Boon, J., Ahlquist, P., 2002. A positive-strand RNA virus replication complex parallels form and function of retrovirus capsids. Mol. Cell 9, 505–514.
Sklan, E.H., Serrano, R.L., Einav, S., Pfeffer, S.R., Lambright, D.G., Glenn, J.S., 2007a. TBC1D20 is a Rab1 GTPase-activating protein that mediates hepatitis C virus replication. J. Bio. Chem. 282, 36354–36361.
Sklan, E.H., Staschke, K., Oakes, T.M., Elazar, M., Winters, M., Aroeti, B., Danieli, T., Glenn, J.S., 2007b. A Rab-GAP TBC domain protein binds hepatitis C virus NS5A and mediates viral replication. J. Virol. 81, 11096–11105.
Smit, C.H., Jaspars, E.M.J., 1982. Evidence that RNA 4 of Alfalfa mosaic virus does not replicate autonomously. Virology 117, 271–274.
Sohn, E.J., Kim, E.S., Zhao, M., Kim, S.J., Kim, H., Kim, Y.-W., Lee, Y.J., Hillmer, S., Sohn, U., Jiang, L., Hwang, I., 2003. Rha1, an Arabidopsis Rab5 homolog, plays a critical role in the vacuolar trafficking of soluble cargo proteins. The Plant Cell 15, 1057–1070.
Spuul, P., Balistreri, G., Kääriäinen, L., Ahola, T., 2010. Phosphatidylinositol 3-kinase-, actin-, and microtubule-dependent transport of Semliki Forest virus replication complexes from the plasma membrane to modified lysosomes. J. Virol. 84 (15), 7543–7557.
Stapleford, K.A., Miller, D.J., 2010. Role of cellular lipids in positive-sense RNA virus replication complex assembly and function. Viruses 2, 1055–1068.
Stone, M., Jia, S., Heo, W.D., Meyer, T., Konan, K.V., 2007. Participation of Rab5, an early endosome protein, in hepatitis C virus RNA replication machinery. J. Virol. 81, 4551–4563.
Targett-Adams, P., Boulant, S., McLauchlan, J., 2008. Visualization of double-stranded RNA in cells supporting hepatitis C virus RNA replication. J. Virol. 82, 2182–2195.
Thole, V., Garcia, M.-L., van Rossum, C.M.A., Neeleman, L., Brederode, F.T., Linthorst, H.J.M., Bol, J.F., 2001. RNAs 1 and 2 of *Alfalfa mosaic virus*, expressed in transgenic plants, start to replicate only after infection of the plants with RNA 3. J. Gen. Virol. 82, 25–28.
Tse, Y.C., Mo, B., Hillmer, S., Zhao, M., Lo, S.W., Robinson, D.G., Jiang, L.X., 2004. Identification of multivesicular bodies as prevacuolar compartments in *Nicotiana tabacum* BY-2 cells. The Plant Cell 16, 672–693.
Ueda, T., Yamaguchi, M., Uchimiya, H., Nakano, A., 2001. Ara6, a plant-unique novel type Rab GTPase, functions in the endocytic pathway of *Arabidopsis thaliana*. EMBO J. 20, 4730–4741.
Van Der Heijden, M.W., Carette, J.E., Reinhoud, P.J., Haegi, A., Bol, J.F., 2001. Alfalfa mosaic virus replicase proteins P1 and P2 interact and colocalize at the vacuolar membrane. J. Virol. 75, 1879–1887.
Van Gisbergen, P.A.C., Esseling-Ozdoba, A., Vos, J.W., 2008. Microinjecting FM4-64 validates it as a marker of the endocytic pathway in plants. J. Microsc. 231, 284–290.

Vlot, A.C., Neeleman, L., Linthorst, H.J.M., Bol, J.F., 2001. Role of the 3′-untranslated regions of Alfalfa mosaic virus RNAs in the formation of a transiently expressed replicase in plants and in the assembly of virions. J. Virol. 75, 6440–6449.
Vonderheit, A., Helenius, A., 2005. Rab7 associates with early endosomes to mediate sorting and transport of Semliki forest virus to late endosomes. PLoS Biol. 3, e233, http://dx.doi.org/10.1371/journal.pbio.0030233.
Wang, X., Lee, W.-M., Watanabe, T., Schwartz, M., Janda, M., Ahlquist, P., 2005. Brome mosaic virus 1a nucleoside triphosphatase/helicase domain plays crucial roles in recruiting RNA replication templates. J. Virol. 79, 13747–13758.
Wei, T., Huang, T.-S., McNeil, J., Laliberté, J.-F., Hong, J., Nelson, R.S., Wang, A., 2010. Sequential recruitment of the endoplasmic reticulum and chloroplasts for plant potyvirus replication. J. Virol. 84, 799–809.